Transactions, SMiRT-25
Charlotte, NC, USA, August 4-9, 2019
Division VIII

A METHOD FOR MONITORING VIBRATIONAL FATIGUE OF STRUCTURES AND COMPONENTS

Nadim Moussallam[1], Rainer Ziegler[2], Steffen Bergholz[3], Jürgen Rudolph[4]

[1]Expert Engineer, Framatome, Erlangen, Germany (nadim.moussallam@framatome.com)
[2]Specialist Engineer, Framatome, Erlangen, Germany
[3]Section Head Engineer, Framatome, Erlangen, Germany
[4]Senior Expert Engineer, Framatome, Erlangen, Germany

ABSTRACT

A vibration fatigue monitoring system has been developed by Framatome to assess, in real time, the evolution of a structure lifetime expectancy. Its originality comes from the fact that only one or a few acceleration measurements are necessary to re-construct the complete stress history in the whole structure, including on welds that could not have been directly instrumented.

The method has been numerically and experimentally validated and the system was successfully installed on a first industrial structure submitted to transient wind loads. It is expected that it will soon find further applications notably in monitoring vibrations induced during NPPs transients that may induce some temporary resonance of piping equipment.

INTRODUCTION

Estimating life duration and preventing fatigue induced failures is a common practice in the design of systems, structures and components. A more advanced practice is to monitor the actual damage accumulation during the structural lifetime based on the real operational loads and a qualified fatigue assessment procedure. This is typically done in some Nuclear Power Plants (NPPs) by constantly recording transient temperatures and stresses at specific sentinel locations in order to capture the amplitudes and number of occurrences of thermal-mechanical stress cycles. Such monitoring approach often allows for a lifetime extension as the number and kind of actually experienced thermal transients is usually lower and less damaging than the ones considered at design stage.

Vibration induced fatigue, on the other side, is almost always excluded at the design stage of NPPs by assuming occurring stress amplitudes below the endurance limit due to appropriate design measures. Still, after a power upgrade or when a NPP starts working in load-following operational mode, there may be some transient phases during which additional vibrations of pipes or other components occur. These transient vibratory phases may induce a certain amount of additional fatigue usage and low-cycle (LCF) – high cycle (HCF) or even very high cycle (VHCF) fatigue interaction, that is to be cumulated in the overall fatigue damage assessment.

To tackle this issue, a vibrational fatigue monitoring system has been developed by Framatome and installed on an industrial structure as a first of the kind. The objective of this system is to assess in real time the evolution of the structure lifetime expectancy.

The system calculates the time history of the elastic stress field in the whole structure based on the information provided by one or a few strategically positioned accelerometers and one or a few displacement or angle sensors. It subsequently assesses the damage status of all welded junctions. The present paper presents (a) the developed methodology to recreate the stress time history within the structure, (b) its theoretical validation on a test structure, (c) an explanation of the stress cycle counting method to assess the cumulative usage factor (CUF) and (d) the on-site application of the complete system.

METHODOLOGY FOR RE-CREATING STRESS TIME HISTORIES

The time history response $\boldsymbol{u}(t)$ of a lightly damped linear mechanical structure to any applied dynamic excitation can always be decomposed as the sum of the *N* responses $q_n(t)$ of its individual eigenmodes $\boldsymbol{\phi_n}$:

$$\boldsymbol{u}(t) = \sum_{n=1}^{N} \boldsymbol{\phi}_n q_n(t) \tag{1}$$

For a mechanical structure discretized in Finite Elements in the form of a mass $\boldsymbol{M}$, stiffness $\boldsymbol{K}$ and damping $\boldsymbol{C}$ matrices, the dynamic equilibrium equation projected onto the modal basis reads:

$$\boldsymbol{\phi}^T \boldsymbol{M} \boldsymbol{\phi}. \ddot{\boldsymbol{q}}(t) + \boldsymbol{\phi}^T \boldsymbol{C} \boldsymbol{\phi}. \dot{\boldsymbol{q}}(t) + \boldsymbol{\phi}^T \boldsymbol{K} \boldsymbol{\phi}. \boldsymbol{q}(t) = \boldsymbol{\phi}^T f_{ext}(t) \tag{2}$$

With $\boldsymbol{\phi}$ the matrix of the modal shapes $\boldsymbol{\phi_n}$, $\boldsymbol{q}(t)$ the vector of the modal responses $q_n(t)$ and $f_{ext}(t)$ the discretized excitation force. This is the basis of the modal superposition method used by analysts worldwide to decompose one large system of coupled equations into *N* uncoupled equations, one for each mode:

$$\ddot{q}_n(t) + 2\xi_n . \omega_n . \dot{q}_n(t) + \omega_n^2 q_n(t) = \frac{\boldsymbol{\phi}_n^T f_{ext}(t)}{\boldsymbol{\phi}^T \boldsymbol{M} \boldsymbol{\phi}} \tag{3}$$

Transferring these equations from the time domain to the frequency domain, the Fourier transform $Q_n(\omega)$ of each mode response can be calculated from the Fourier transform of the projected excitation force $P_n(\omega)$ and the mode transfer function $H_n(\omega)$:

$$Q_n(\omega) = H_n(\omega) . P_n(\omega) \tag{4}$$

$$H_n(\omega) = [-\omega^2 + 2i\omega\omega_n\xi_n + \omega_n^2]^{-1} \tag{5}$$

$$P_n(\omega) = \int_{-\infty}^{+\infty} \frac{\boldsymbol{\phi}_n^T f_{ext}(t)}{\boldsymbol{\phi}^T \boldsymbol{M} \boldsymbol{\phi}} e^{-i\omega t} dt \tag{6}$$

$$Q_n(\omega) = \int_{-\infty}^{+\infty} q_n(t) e^{-i\omega t} dt \tag{7}$$

With ω_n the modal circular frequency of the nth mode and ξ_n its modal damping. Finally, the Fourier transform $\boldsymbol{U}(\omega)$ of the time history response $\boldsymbol{u}(t)$ can be expressed as the sum of the Fourier transform of the modal responses $Q_n(\omega)$:

$$\boldsymbol{U}(\omega) = \sum_{n=1}^{N} \boldsymbol{\phi}_n Q_n(\omega) \tag{8}$$

The dynamic response of a linear structure to a broadband random excitation, such as the one exerted by wind or by fluid turbulence, include the response of all its modes in the complete excitation frequency range. As $P_n(\omega)$, in equation (6), generally varies only slowly as a function of ω while $H_n(\omega)$, in equation (5), present sharp peaks in the vicinity of the mode resonant frequency ω_n, the bulk of each mode response energy will effectively be concentrated around ω_n. This is also true for a structure transient response to an impulsive load, such as an impact, a fluid hammer or a pressure wave. Therefore, in all these cases a reasonable estimate of the response Fourier transform can be defined as:

$$\boldsymbol{U}(\omega) \approx \sum_{n=1}^{N} \boldsymbol{\phi}_n Q_n(\omega) B_n(\omega, \omega_n) \tag{9}$$

with $B_n(\omega, \omega_n)$ a bandpass filter function in the frequency range of influence of the nth mode around ω_n. If the modes are well separated from each other and their influence range in the frequency domain do no significantly intersect, the single mode response $Q_n(\omega)$ can in turn be estimated from the Fourier transform $\ddot{U}_m(\omega)$ of a single acceleration record at a single point m of the structure:

$$Q_n(\omega) \approx \frac{\ddot{U}_m(\omega).B_n(\omega, \omega_n)}{-\omega^2 \phi_{nm}} \tag{10}$$

with ϕ_{nm} the nth mode shape value at point m. The displacement Fourier transform $\boldsymbol{U}(\omega)$ at all points of the structure can then be deduced from equation (8), by modal superposition knowing the modal responses $Q_n(\omega)$. The response time history $\boldsymbol{u}(t)$ can be obtained by an inverse Fourier transform of $\boldsymbol{U}(\omega)$. Knowing $\boldsymbol{u}(t)$, it is then relatively straightforward to deduce the time history deformation force field time history $\boldsymbol{K}.\boldsymbol{u}(t)$ in the structure and to deduce from it the stress tensor time history $\boldsymbol{\sigma}(t)$ at all locations of interest for the fatigue analysis.

NUMERICAL VALIDATION AND ADDITION OF PSEUDO-STATIC CORRECTION

A finite element model of an industrial tower was built to test the complete methodology. This model is illustrated Figure 1 a). A single recording point is set near the top of this structure. At this altitude, the acceleration in both horizontal directions is recorded by two accelerometers and the rotation angles of the tower are recorded by two inclinometers. The modal basis of the structure is presented in Figure 1 b) and 1 c) with a normalization at the recording point.

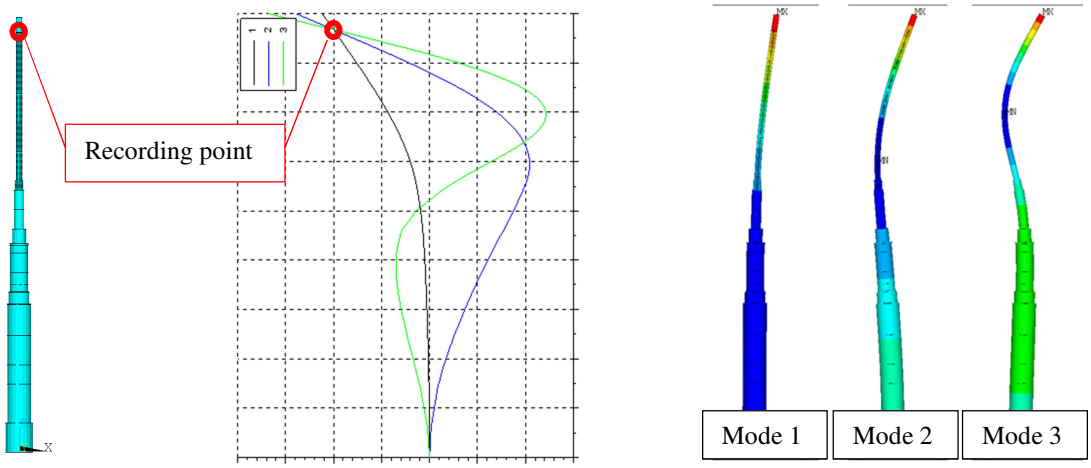

a) b) c)

Figure 1. Test model of an industrial chimney a) Finite element model, b) Modal basis normalized to the recording point, c) Illustration of the first three modes

This model is submitted to two different fields of random excitations in the X and Y directions. These excitations are synthetic time signals generated to represent two different kinds of wind loads: the complete structure height is excited in X, triggering a response mainly on the first mode, while only the upper part is excited in Y, triggering a response mainly on the third mode. The partial excitation is representative of a tower partly protected from wind loads by an adjacent building. The responses to these excitations, as recorded at the top location, are illustrated in Figure 2. From the acceleration records of Figure 2, noted $\ddot{u}_m(t)$, acceleration Fourier transforms $\ddot{U}_m(\omega)$ are calculated and then displacement Fourier transforms $U_m(\omega) = -\ddot{U}_m(\omega)/\omega^2$. These displacement Fourier transform are illustrated Figure 3, keeping the same colors to identify the X and Y directions.

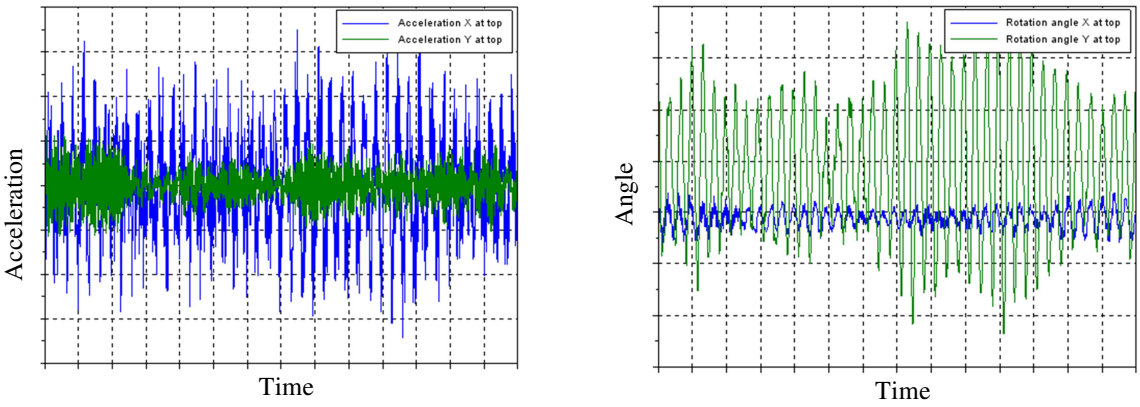

Figure 2. Records in X (blue) and Y (green) directions at the structure selected recording point

Starting from $U_m(\omega)$ and applying the methodology detailed in the first part of this paper, the modes responses in frequency domain $Q_n(\omega)$ and in time domain $q_n(t)$ can be reconstructed. The displacement field $\boldsymbol{u}(t)$ in the complete structure is then obtained through equation (1) by superposing the contribution of each mode. As an illustration of this process, Figure 4 gives the separated modal contributions of modes 1 to 3 to the time history displacement at the structure top point.

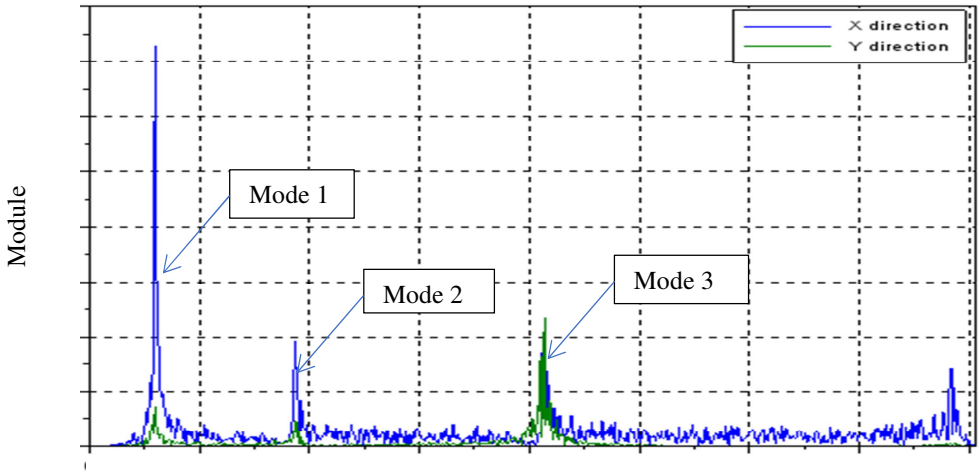

Figure 3. Displacement Fourier transform at the recording point in X (blue) and Y (green) directions

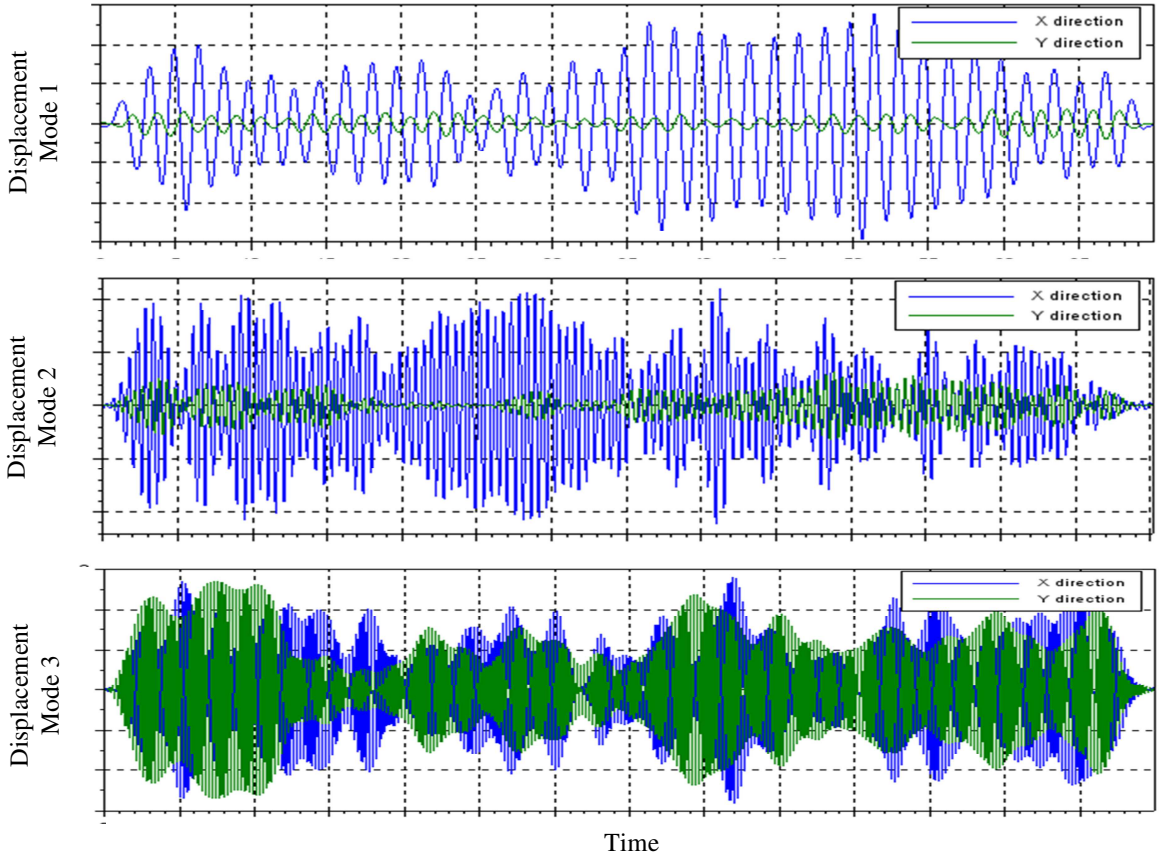

Figure 4. Contribution of each mode to the displacement at the structure top

Additionally to the dynamic movement of the structure, there might be a pseudo-static response to the excitation. Typically, a wind load in a given direction and with a given amplitude leads to oscillations of the tower around a position that does correspond to its static response to this load. This static response changes as a function of the wind direction and intensity, producing a pseudo static

displacement field that does influence the stress time histories within the structure. As the pseudo-static motions are very slow, they are generally difficult to accurately capture with acceleration sensors. To this aim, an additional type of measurement is added: displacement sensors or, in the case of the test structure, inclination sensors. The measured displacement or angle at a representative point of the structure is compared to the reconstructed displacement or angle at the same point, based on the modal superposition resulting from accelerometer records. The difference is then applied as a pseudo static correction function to the entire displacement field. This process is illustrated Figure 5.

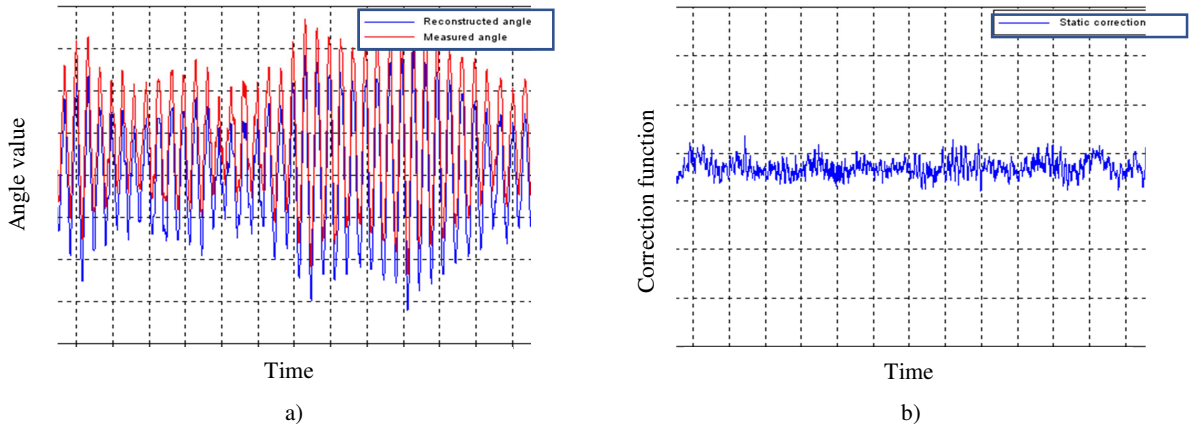

Figure 5. Pseudo-static correction process a) difference between measured and calculated displacement and b) corrective function

Finally, and for verification purposes, the "reconstructed" stress field is compared to the stress field directly calculated with the time history analyses at several positions representative of the sensitive welds of the test structure. As shown in Figure 6 for two different locations, there is an excellent fit.

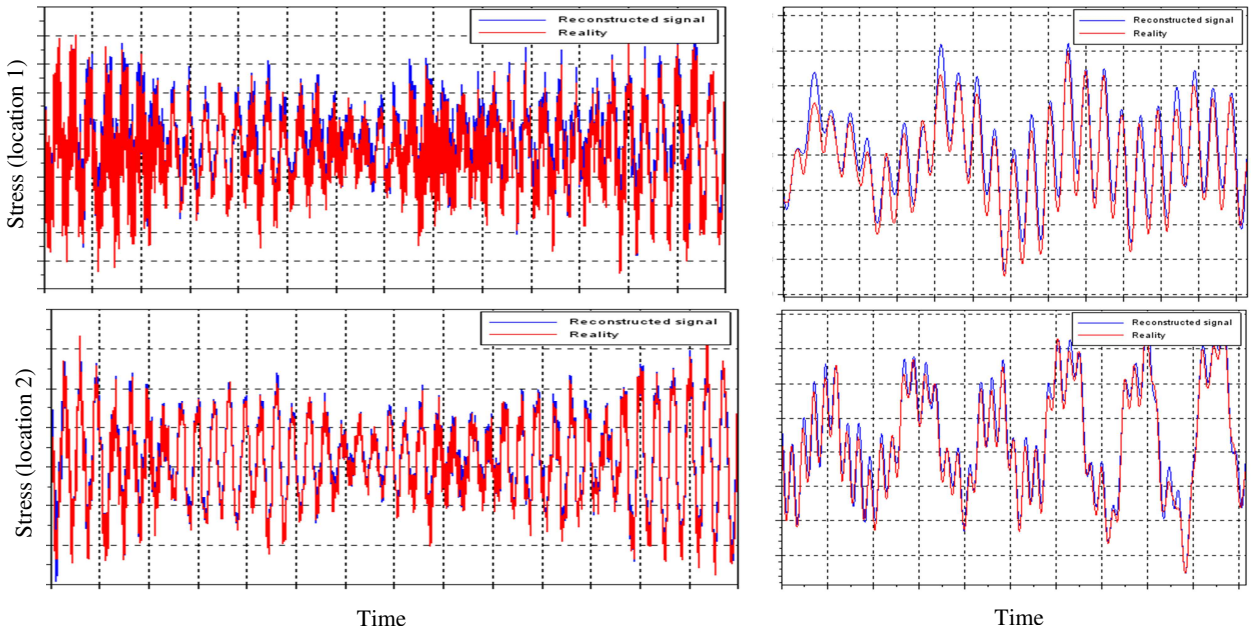

Figure 6. Comparison of directly calculated stresses (in red) and reconstructed stresses (in blue) for two locations

STRESS CYCLE COUNTING AND CALCULATION OF CUMULATIVE USAGE FACTOR

Knowing the stress tensor time history $\boldsymbol{\sigma}(t)$, a rainflow cycle counting algorithm is applied. This method is described in Matsuishi and Endo (1968). Amongst different available procedures, the Hysteresis Counting Method (HCM) according to Clormann and Seeger (1986) is proposed as the most appropriate variant of the rainflow counting algorithm for arbitrary series of loads / stresses as a function of time respectively data point pairs. The algorithm is capable of efficiently counting ranges (amplitudes) and mean values (if required) of one variable (e.g. temperature, stress or strain components). The algorithm implies a Masing-memory model, see Masing (1926), and counts every single closed cycle. The algorithm can easily be implemented according to the flowchart given in figure 7.

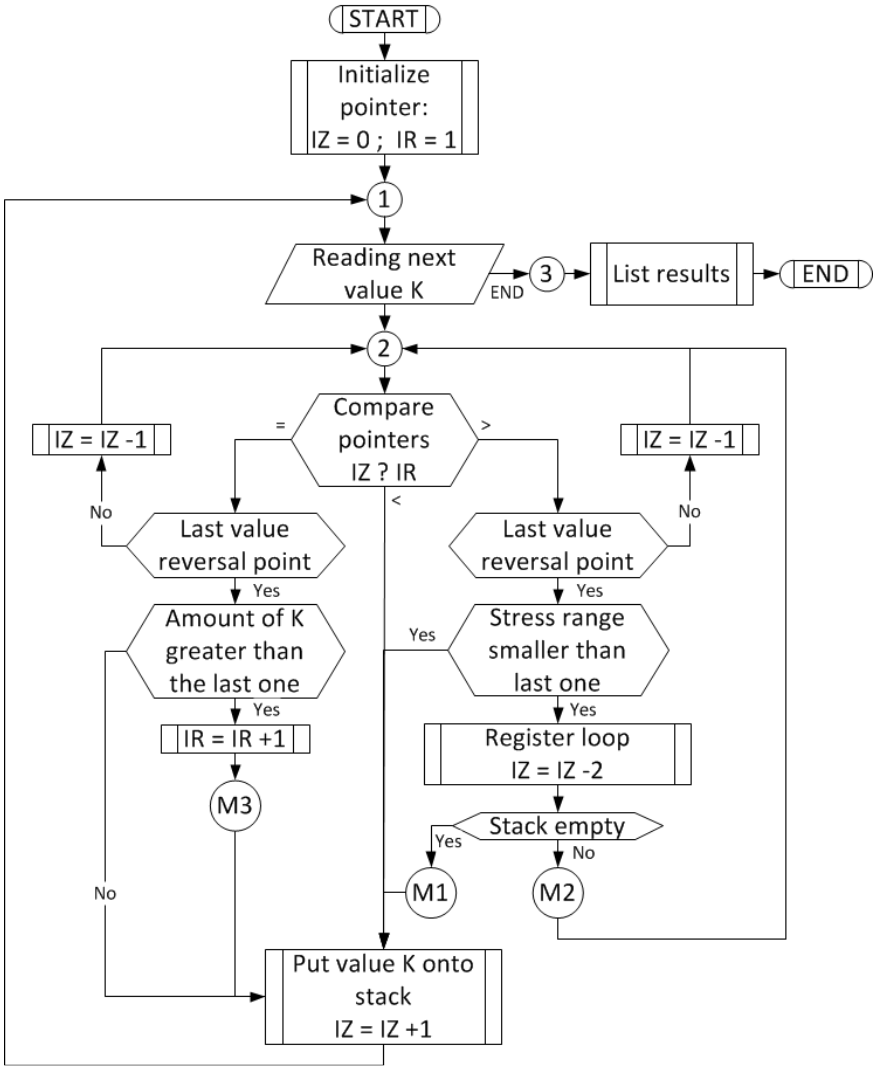

Figure 7. Flow chart of the Rainflow cycle counting method, according to Clormann and Seeger (1986)

However, HCM is a single parameter counting method. Hence, there are several options of parameters to be counted depending on the fatigue damage model applied. For a design code conforming calculation the procedure described in Rudolph et al (2019), without integrating a critical plane approach, the following steps are to be implemented: a) Cycles are counted based on the variation of each stress component (σ_{xx}, σ_{yy} , σ_{zz} , σ_{xy}, σ_{yz}, σ_{xz}) separately. b) A fatigue analysis is performed based on the range of equivalent stress (Tresca or von Mises) range of each cycle. This results in a different cumulative usage factor (CUF) depending on which stress component is used to count the cycles. c) The fatigue assessment is based on the cycles of the stress component leading to maximum fatigue damage.

This means that the time histories of all six stress components (σ_{xx}, σ_{yy} , σ_{zz} , σ_{xy}, σ_{yz}, σ_{xz}) are consecutively used as the counting parameters. The equivalent stress ranges (Tresca or von Mises) relating to the cycles are calculated and used for the determination of partial usage factors. The total cumulative usage factor CUF is the linear damage summation (Miner's rule). The worst case CUF resulting from the six cycle-counts applies. Fatigue damage is calculated cycle by cycle. More advanced damage parameters may be used in combination with a critical plane approach. These specific approaches are not discussed in further detail here.

ON-SITE APPLICATION

The fatigue vibration monitoring method described in the previous chapters was implemented as a complete system on an industrial structure subjected to wind loads. The system included sensors, recorders and servers hosting a specifically developed software that implements the previously described methodology. Every 5 minutes, the software re-assesses the fatigue state in each of the sensitive weld locations of the structure and updates the life duration estimate accordingly.

Additionally to the system, and for verification purposes, strain gages were installed at several positions on the structure outer surface. The objective of these strain gages was to provide a direct assessment of the stresses at specific locations. These "measured" stresses are then systematically compared to the "reconstructed" ones in terms of number and amplitude of experienced load cycles. Figure 8 gives an example of such comparison at a given location and is representative of the results obtained everywhere else. The "measured" and "reconstructed" stress signals are not fully identical due on one side to the several steps of signal processing performed to reconstruct the signal and on the other side on the measurement noises at high frequencies in both the strain and the acceleration recordings. Nevertheless, the number of load cycles, their amplitude and their history of occurrence is perfectly reproduced in the "reconstructed" signal.

The usage factor of each welded junction is re-evaluated every 5 minutes and made accessible to the plant owner through an interface. As an example, Figure 9 shows the evolution of the usage factor for a period of a few months. During this period, only two storms have generated a stress level sufficient to induce a variation of the usage factor.

Finally, Figure 10 shows the history of loads in terms of RMS displacements at the top of the structure on a duration of a few days. The contribution of each mode is plotted in color and the overall displacement in black. In this case, the first mode clearly dominates the response.

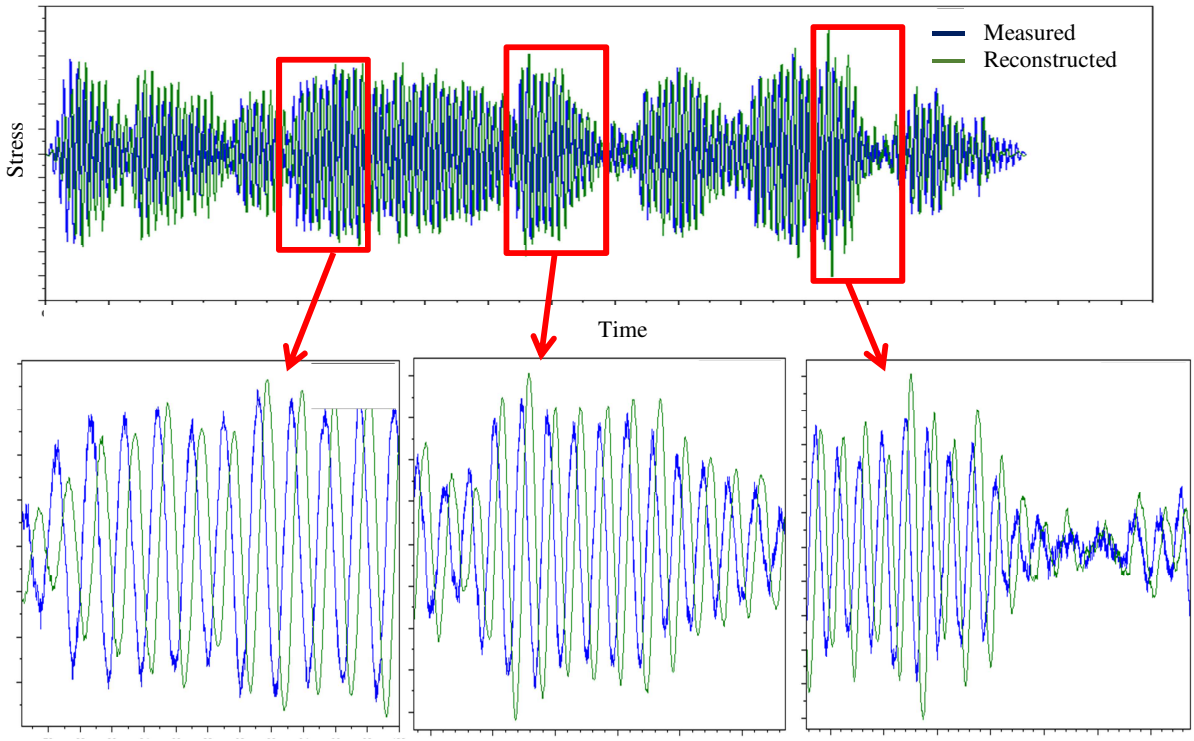

Figure 8. Comparison of measured (blue) and reconstructed (green) stress time history at one example location of the structure

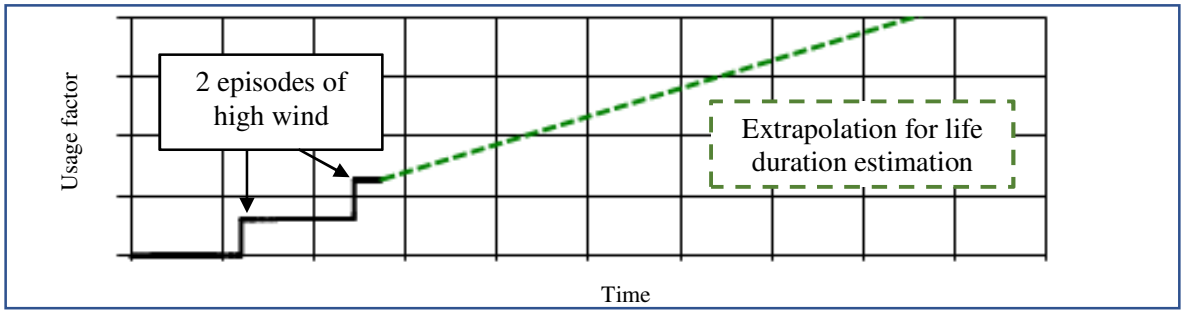

Figure 9. Follow up of usage factor and life duration estimation

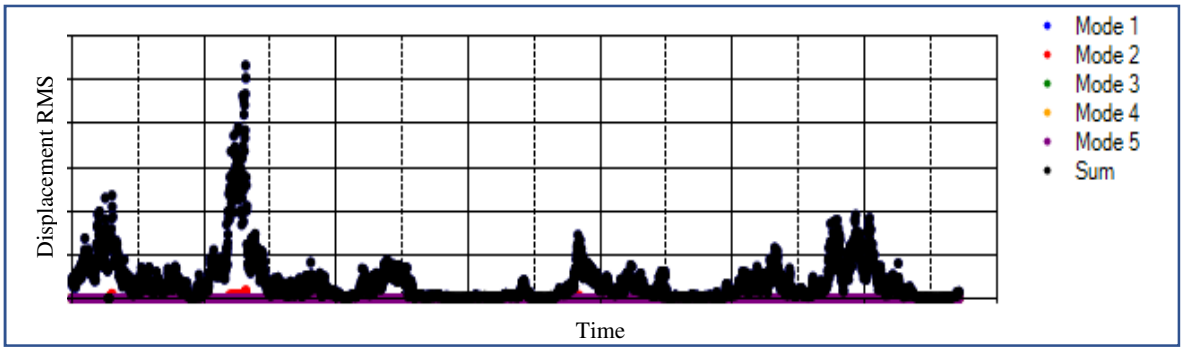

Figure 10. History record of RMS displacement and decomposition per modes

CONCLUSION

A method for reconstructing stress time histories everywhere in structure dynamically responding to external or internal broad band excitation has been validated numerically and experimentally. From these stress time histories, a best estimate of the usage factor can be calculated at each point of interest and a life duration estimate can be updated in real time.

Although the first structure for which the Framatome vibratory fatigue monitoring system has been implemented is an industrial tower subjected to wind loads, it is expected that the next applications will be in the nuclear sector. Especially, it is foreseen to monitor some pipes subjected to transient vibratory loads in combination with thermal loads. Hence, this monitoring could also be coupled to a monitoring of thermal transient loads, which are captured by a similar principle but based on measurement sections of thermocouples.

REFERENCES

Clormann, U. H., Seeger, T. (1986). *Rainflow – HCM Ein Zählverfahren für Betriebsfestigkeitsnachweise auf werkstoffmechanischer Grundlage*. Stahlbau 55, no. 3, pp. 65/71

Masing, G. (1926). *Eigenspannungen und Verfestigung beim Messing*. Proceedings of the 2nd International Congress of Applied Mechanics. Zürich, pp. 332–335.

Matsuishi, M., Endo, T. (1968). *Fatigue of metals subjected to varying stresses*. Proc. Kyushu Branch of Japan. Soc. of Mech. Eng., S. 37/40

Rudolph, J., Baylac, G., Trieglaff, R., Gawlick, R., Krämer, M., Simonet, Y., Triay, M. (2019). *Outline of the Recent Consolidated Revision of EN13445-3, Clause 18 and Related Annexes: Detailed Assessment of Fatigue Life*. PVP2019-93910. Proceedings of the ASME 2019 Pressure Vessels and Piping Conference PVP2019, July 14-19, 2019, San Antonio, Texas, USA